A Micro-Scale Biosensor for the Detection of Bacillus Stearothermophilus Spore Germination

M.İ. BEYAZ[1] and A. SEKKOUTI[1]

[1] Antalya Bilim University, Antalya/Turkey, mibeyaz@antalya.edu.tr
[1] Antalya Bilim University, Antalya/Turkey, aissa.sekkouti@antalya.edu.tr

***Abstract* – Germination of Bacillus Stearothermophilus bacterial spores is being used as a marker in sterilization monitoring systems to verify the success of sterilization processes in healthcare facilities. Such systems mainly employ optical detection techniques that are expensive and time consuming. This work presents the first micro-scale biosensing platform that is capable of detecting this specific spore germination through impedance measurements. Starting from theoretical calculations on ion concentrations, a simulation model is built on COMSOL software to analyze the conductance change of the medium during germination. It has been demonstrated that even 1% germination ion yield results in a 5-fold drop in germinant solution resistance, reaching up to more than two orders of magnitude decrease when the spores are fully germinated. A microfluidic biosensor consisting of interdigitated electrodes was designed, and a fabrication approach has been presented. This device, when fully fabricated, poses an inexpensive solution that can provide sterilization verification results in under 10 minutes.**

***Keywords* – Biosensor, impedance, MEMS, lab on a chip, germination**

I. Introduction

HEAT based sterilization is a procedure frequently applied in healthcare facilities as a means to eliminate harmful organisms on medical tools. The procedure involves locating each medical tool in an oven and applying dry or wet heat at temperatures exceeding 120 °C for up to one hour. It is vitally important to ensure that such tools are completely cleaned and free of bacteria before getting in contact with the next patient. To this end, Bacillus Stearothermophilus non-pathogenic bacterial spores provide a reliable marker for the success of sterilization [1-3]. These spores are known to be one of the most heat resistant organisms [2], and are heavily used in temperature-related biological studies. During the sterilization process, these spores are simultaneously located in sterilization ovens together with other medical tools. Following the end of the process, the spores are placed in a nutrient solution at an optimal temperature to observe whether germination will occur. If the spores do not germinate into functional bacteria, this shows that the heat-resistant spores have been killed during sterilization, which indirectly demonstrates that all other bacteria on the medical tools are also eliminated since they are less heat resistant than these spores. The germination of the spores into bacterial form, on the other hand, shows that these spores and possibly other harmful bacteria on the tools were not successfully exterminated.

The germination of the Bacillus Stearothermophilus spores are currently detected using optical methods. In this respect, the spores are encapsulated in small indicators with nutrient solutions, and placed in incubators that provide optimal conditions for germination. The incubators include a UV light source together with photodiodes and electronics to detect fluorescence photon emission. The spores are exposed to UV light, which leads to fluorescence emission in the presence of germination. Read out electronics detect this phenomenon and the result is displayed on a small screen. Depending on the indicator and incubator used, the detection may take between 0.5 – 4 hours. In addition such indicators and incubators are expensive, prohibiting their wide availability in all healthcare facilities.

In this work, we present the analysis and design of an inexpensive micro-scale biosensor that can detect the germination faster than current incubators. The germination cycle of these specific spores leads to ion exchange between the spore and outside medium in 5 minutes after the start of germination [4-7]. This shows that the germination can be detected in 5-10 minutes by monitoring the conductance of the medium. Such impedance based biosensing of various biological agents have been demonstrated previously in the literature [8-10]. However, to the best of our knowledge, this is the first study on the development of a biosensor tailored for this specific bacterial spores. The sensor is designed using MEMS and lab on a chip technologies to minimize the system cost and detection time as well as to reduce the sample volume.

II. Analysis and Design

The spore mineral content mainly includes dipicolinic acid (DPA), calcium, magnesium, manganese, potassium, and sodium, which are released at different phases of germination. [11-14]. Among these minerals, the highest mineral concentration belongs to DPA, and followed by calcium, and manganese as summarized in Table 1-2 [15].

Table 1: The mineral content of the spores

Content (μmol/mg [dry weight] of spores)					
DPA^{2-}	Ca^{2+}	Mn^{2+}	Mg^{2+}	K^{+}	Na^{+}
83.1	0.92	0.05	0.05	0.02	0.01

Table 2: The percentage of each ion in single spore dry weight

% dry weight of a single native spore					
DPA^{2-}	Ca^{2+}	Mn^{2+}	Mg^{2+}	K^{+}	Na^{+}
26.4	2.5	1.4	0.24	0.8	0.1

Based on the amount of each ion existing in the spore, the molar ion charge density, σ_c, have been calculated using

$$\sigma_c = e \times z \times c \times N_A \quad (1)$$

where e is the unit charge, z is the number of charges of each ion, c is the concentration of each ion calculated using the above tables, and N_A is the Avogadro's number. The calculated charge densities are listed in Table 3.

Table 3: Calculated ion charge densities

Charge density in $C/m^3 \times 10^6$					
DPA^{2-}	Ca^{2+}	Mn^{2+}	Mg^{2+}	K^+	Na^+
-11.23	0.27	0.07	0.02	0.001	0.01

The resulting charge densities in Table 3 show that the DPA^{2-} is the dominant ion released outside the spore during the germination, and other ions can be fairly neglected to decrease the complexity of the following model. Based on this analysis, the ionic conductivity introduced by the DPA^{2-} is calculated using Einstein relation that describes the relationship between an electrolyte molar conductivity and the diffusion coefficient of the ion content. Accordingly, the molar ionic conductivity, λ, can be written as

$$\lambda = z^2 \times D \times F^2 / R \times T \quad (2)$$

where F is the Faraday constant, R is the gas constant, T is the thermodynamic temperature, and D is the diffusion coefficient that can be calculated as

$$D = k \times T / 6\pi \times \eta \times a \quad (3)$$

In this equation, k represents the Boltzmann constant, η is the viscosity of the medium (in this case germinant solution, or equivalently, water), and a is the radius of the DPA^{2-} [16]. All the parameters of equations (2-3) are known except the DPA^{2-} radius. The DPA crystal contains two molecules whose volume is 0.338 nm^3 [16]. At this point, a fair assumption is made, where this molecule has a spherical geometry and its radius can be found by using the volume of a simple sphere. Accordingly, the radius of the DPA^{2-} was calculated to be 0.343 nm. Therefore, the molar conductivity of the germinant solution containing DPA2- was determined to be 107.3 $S \times cm^2/mol$. Assuming the worst scenario, where one droplet (0.05 ml) of germinant solution on a 1 cm^2 sensor surface results in only 10% of the spores covering the device surface, and only 10% of those spores germinate, equating a DPA yield of 1%, this value translates into a solution conductivity increase of 7.725 mS/m.

The significant increase in solution conductance can be detected using a biosensor with on-chip electrodes that can perform conductivity or resistance measurements. The general sensor configuration is shown in Fig. 1.

The device mainly consists of a set of two electrodes on an insulating substrate that measures slightly larger than 1 cm^2 in area. Although not shown in Fig. 1, the electrodes are designed in interdigitated structure, and embedded in a microfluidic chamber to perform resistance measurements. A droplet of germinant solution also containing cylindrical-shaped bacterial spores are dispensed on the electrodes. The resistance of the medium is measured by applying a voltage and reading the resulting current between the electrodes. The detailed electrode design is shown in Fig. 2, where each electrode consists of 119 thin and long finger lines measuring 150 nm × 20 μm × 8.25 mm in thickness, width, and length, respectively. The fingers reaching to the left and right sides are connected together. This interdigitated design has been preferred over simpler electrode structures to provide a larger electro-active area for interaction, and to decrease the resistance values to an easily detectable range for readout electronics. The finger interspacing has been selected as 20 μm to decrease the microfabrication complexity.

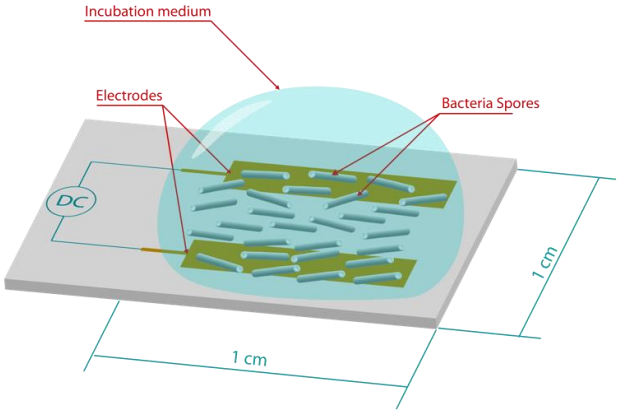

Figure 1: General biosensor design that shows the sensing principle. Electrodes are not drawn in detail for image clarity.

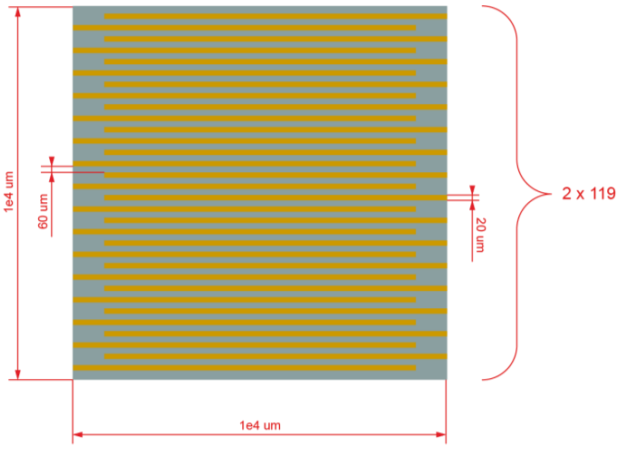

Figure 2: Detailed design of interdigitated electrodes. All the thin fingers reaching to the left and right are connected together.

III. Device Performance

The conductivity change of the germinant solution determined through the analysis presented above leads to the change in solution resistance. Since the electrodes are thin and long, their surface to volume ratio is quite high, which is observed in all devices designed in the realm of MEMS. Therefore, a simple calculation on resistance is not possible as the fingers have many edge areas, where the current density becomes higher than the rest of the electrode structure. This non-linear structure is investigated using COMSOL simulation software that can perform finite element analysis on electric currents. Specifically, the AC/DC module with Electric Current physics have been

used to model the problem. The electrode structure is drawn and a potential difference is applied. The software determines the current density throughout the device and calculates the resulting resistance. Figure 3 shows an example simulation output demonstrating that the current density is higher along the top edge of the interdigitated fingers.

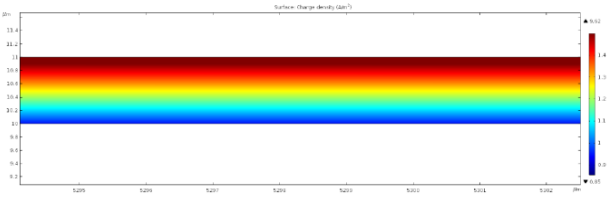

Figure 3: Current density simulation results showing the current is higher along the top edge of the interdigitated electrodes

Next, the resistance of the germinant solution has been calculated in the simulations for the cases when (i) no germination exists, (ii) germination with varying DPA2- yields. It has been demonstrated that when there is no germination, the germination solution that consists of L-alanine and inosine results in a total resistance of 320 Ω. Figure 4 below shows the decreasing resistance of the germinant solution as a result of the DPA^{2-} release during germination.

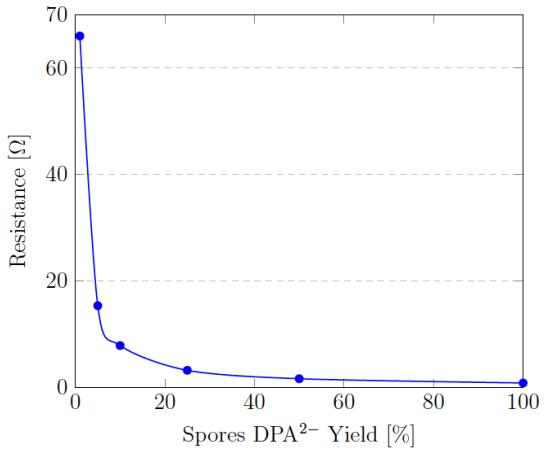

Figure 4: Decreasing trend of the solution resistance as a result of DPA^{2-} released during germination.

The resistance of the solution decreases to 66 Ω when there is only 10 % of chip area coverage and when only 10 % of the spores germinated, which was recalled as 1% DPA yield as described above. Accordingly, even this very small percentage of germination results in the resistance to drop from 320 Ω to 66 Ω, showing a 5 fold decrease in resistance. This effect is easily observable by using simple readout electronics that can perform resistance measurements. The decreasing resistance effect has been further investigated by assuming different levels of spore coverage and germination, leading to increasing DPA yields. Figure 4 shows that the resistance can decrease down to less than 1 Ω when the DPA yield is 100%, showing an even pronounced two orders of magnitude change in resistance. Considering that even small amounts of DPA can be easily observed, and that the DPA release starts in the first five minutes of germination, the results illustrated in Fig. 4 indicate that the germination of these spores can be detected in less than 10 minutes.

IV. Biosensor Fabrication

The biosensor structure presented in this work has feature sizes down to micrometers. Accordingly, microfabrication technology is required to manufacture the device. The process flow designed for this biosensor is summarized in Fig. 5.

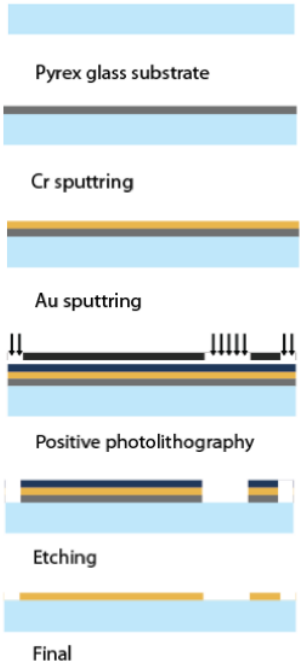

Figure 5: Microfabrication process flow for the biosensor

The device is designed to be fabricated on an insulating pyrex substrate that provides bottom electrical isolation. Initially a 50 nm-thick Cr layer will be sputtered on the substrate that will act as an adhesion layer between the Au and pyrex. Next, 100 nm-thick Au layer will be sputtered as the main electrode layer to interact with the spores and germinant solution. Au is specifically selected to prevent possible electrode corrosion due to extended exposure to germinant solution. At this point, Au electroplating to further increase the electrode thickness can be an option to decrease the internal electrode resistance and increase signal to noise ratio during resistance measurements. Following Au deposition, positive photolithography with the electrode on a mask pattern will be applied. Next, wet etching of Cr and Au will be performed sequentially. Finally, the remaining photoresist will be removed in acetone and the device fabrication will be finished. The current efforts are focused on performing this fabrication flow and demonstrating the first set of devices.

V. Conclusion

A biosensor that can detect the germination of Bacillus Stearothermophilus bacterial spores is presented. The device

is composed of interdigitated electrode structures integrated in a microfluidic chamber on an insulating substrate. Our design and simulations show that ion yield as low as 1% results in a 5 fold decrease in resistance, which can be easily detected by readout electronics. Further analysis demonstrated that the resistance can change more than two orders of magnitude when the spores are fully germinated, pointing out the suitability and applicability of the device. A fabrication process flow to manufacture the device was presented. Current efforts are focused on microfabricating the biosensors for testing and evaluation. The sensor structure presented in this work will enable the development of a low-cost sterilization monitoring device that can perform the process verification in less than 10 minutes.

REFERENCES

[1] D. Greenwood, R. C. Slack, M. R. Barer, and W. L. Irving, *Medical microbiology e-book: a guide to microbial infections: pathogenesis, immunity, laboratory diagnosis and control.* Elsevier Health Sciences, 2012.

[2] M. P. Doyle and R. L. Buchanan, *Food microbiology: fundamentals and frontiers.* American Society for Microbiology Press, 2012.

[3] C. Rigaux, S. Andre, I. Albert, and F. Carlin, "Quantitative assessment of the risk of microbial spoilage in foods, prediction of non-stabiliy at 55 c caused by geobacillus stearothermophilus in canned green beans," *International Journal of Food Microbiology*, vol. 171, pp. 119-128, 2014

[4] D. Xu and J. C. Cote, "Phylogenetic relationships between bacillus species and related genera inferred from comparison of 3 end 16s rdna and 5 end 16s-23s its nucleotide sequences," *International Journal of Systematic and Evolutionary Microbiology*, vol. 53, no. 3, pp. 695-704, 2003.

[5] "Bacillus stearothermoophilus bacteria spore, MicrobeWiki, https://microbewiki.kenyon.edu/index.php/Bacillus_stearothermophilus_NEUF2011, Accessed 2019-09-01.

[6] K. Reineke, "Mechanism of bacillus spore germination and inactivation during high pressure processing," Ph.D. dissertation, Technischen Universitat Berlin, Berlin, Germany, 2012.

[7] P. Setlow, "Spore germination," *Current Opinion in Microbiology*, vol. 6, no. 6, pp. 550-556, 2003.

[8] L. Yang, Y. Li, and C. F. Erf, "Interdigitated array microelectrode-based electrochemical impedance immunosensor for detection of Escherichia coli o157: H7," *Analytical Chemistry*, vol. 76, no. 4, pp. 1107-1113, 2004.

[9] Y. S. Liu, T. Walter, W. J. Chang, K. S. Lim, L. Yang, S. Lee, A. Aronson, and R. Bashir, "Electrical detection of germination of viable model bacillus anthracis spores in microfluidic biochips," *Lab on a Chip*, vol. 7, no. 5, pp. 603-610, 2007.

[10] S. Kim, G. Yu, T. Kim, K. Shin, and J. Yoon, "Rapid bacterial detection with an interdigitated array electrode by electrochemical impedance spectroscopy," *Electrochimica Acta*, vol. 52, pp. 126-131, 2012.

[11] R. S. Thomas, "Ultrastructural localization of mineral matter in bacterial spores by microincineration," *The Journal of Cell Biology*, vol. 23, no. 1, pp. 113-133, 1964.

[12] H. R. Curran, B. Brunstetter, and A. Myers, "Spectrochemical analysis of vegetative cells and spores of bacteria," *Journal of Bacteriology*, vol. 45, no. 5, pp. 485, 1943.

[13] J. F. Powell and R. Strange, "Biochemical changes occurring during sporulation in bacillus species," *Biochemical Journal*, vol. 63, no. 4, pp. 661, 1956.

[14] V. Vinter, "The effect of cystine upon spore formation by bacillus megaterium," *Journal of Applied Bacteriology*, vol. 20, pp. 325, 1957.

[15] T. C. Beaman, H. S. Pankratz, and P. Gerhardt, "Heat shock affects permeability and resistance of bacillus stearothermophilus spores," *Applied and Environmental Microbiology*, vol. 54, no. 10, pp. 2515-2520, 1988.

[16] A. Sekkouti, "A theoretical study and a micro-scale sensing platform for the detection of germination in bacillus stearothermophilus spores," Ms. Thesis, Department of Electrical and Electronics Engineering, Antalya Bilim University, Antalya, Turkey, 2019.